Surface Stoichiometry and the Initial Oxidation of NiAl(110)

Alexander Y. Lozovoi, Ali Alavi, and Michael W. Finnis
Atomistic Simulation Group, School of Mathematics and Physics, Queen's University, Belfast BT7 1NN, United Kingdom
(Received 21 March 2000)

Selective oxidation of the surface of an ordered alloy requires redistribution of the atomic species in the vicinity of the surface. This process can be understood in terms of the formation and movements of point defects in the compound. On the basis of *ab initio* density-functional calculation we found both the creation of exchange defects near the NiAl surface and segregation of Ni vacancies to the top layer to be extremely favorable in the presence of oxygen. Scenarios for the initial oxidation of NiAl are suggested which demonstrate the appearance of an additional energy barrier on the Ni-rich side compared to the Al-rich side. The expulsion of Ni from the oxide layer as it forms is the driving force for its stability.

PACS numbers: 68.35.Md, 68.35.Dv, 71.20.Lp, 81.15.Aa

The oxidation of metal surfaces is relevant to many fields in which the metal-oxide interface occurs, including heterogeneous catalysis and corrosion. Understanding the microscopic processes which govern the *initial* stages of oxidation has been the focus of much research recently, using both experimental and theoretical *ab initio* techniques. The oxidation of *pure* metal surfaces such as Al(111) is comparatively well understood [1,2]; however, the situation in metallic *compounds* is much less clear, even though the latter are of great practical importance. For example, the intermetallic NiAl, which is prototypical of highly ordered metallic compounds, easily oxidizes, forming a continuous coherent Al_2O_3 film (about 5 Å thick) (see Ref. [3] for a review). This property is widely used in growing well-ordered alumina films for experimental investigation; for that purpose NiAl is better suited than pure Al, as the low melting temperature of the latter makes it impossible to obtain films of well-ordered alumina in its stable configuration [3]. In particular, Al_2O_3/NiAl(110) is considered to be one of the most convenient model systems for experimental studies of alumina supported metallic nanoclusters [4].

The structure of the oxide film on the NiAl(110) surface is described as follows: at low temperatures the film is amorphous (locally ordered), at higher temperatures (about 1300 K) it becomes globally ordered and takes on the structure of two O-Al bilayers, terminated with an Al layer on the interface and with an O layer from vacuum [5–7]. According to [7], the NiAl-Al_2O_3 interface is atomically sharp without any intermediate phases. The possibility of Ni-O bond formation in either low-temperature or high-temperature oxide is doubted [6–8]. The presence of "metallic" Ni at the oxidized surface at low temperatures has not been ruled out, but during the higher temperature annealing Ni atoms are suggested to be expelled from the ordering oxide overlayer [6].

In the absence of an atomic-scale mechanism of the film formation, one cannot explain the observed oxygen uptake curves [8], nor resolve whether the oxidation *injects* additional vacancies into the NiAl crystal by extracting Al atoms [9], or, on the contrary, *absorbs* vacancies by destroying a few surface layers of NiAl with subsequent dissolution of Ni atoms in the bulk [6].

Here we present the first detailed *ab initio* study of the oxidation of NiAl(110), and show that qualitatively new phenomena occur, when compared to pure metal surfaces, in the oxidation process. These are related to the additional thermodynamic degree of freedom available, namely the composition of the surface. We show that the thin oxide film is hugely stabilized by the introduction of *point defects* at the surface, in particular, Al antisites and Ni vacancies. Based on these observations, we develop scenarios involving segregation of point defects to the surface as a result of the oxidation. An implication of this is that the change of point defect thermodynamics in the *bulk* in crossing the stoichiometric composition, significantly affects the oxidation at the *surface*. As a result, the kinetics of the oxidation process for Ni-rich and Al-rich alloys will be different. Such an effect should be present in the oxidation of any ordered compound that requires redistribution of the species [10].

Calculations were performed using the plane wave pseudopotential method within the framework of the finite-temperature density functional theory [11]. The surface of NiAl was modeled by a slab consisting of four layers separated with four interlayer spacings of vacuum; atoms of the two bottom layers of the slab were held fixed at their bulk positions. Each layer contained four nonequivalent atomic positions, as shown in Fig. 1. For the Brillouin zone integration the $4 \times 4 \times 2$ Monkhorst-Pack mesh was employed. We used soft kinetic-energy-filtered pseudopotentials for Ni and O [12] (for Al, we used the Troullier-Martins pseudopotential [13]) and the electronic orbitals were expanded up to a cutoff of 50 Ry.

Geometry optimizations were performed until the maximal force component dropped below 1 mH/a.u. As a rule, atomic arrangements with which we dealt had a complicated energetic surface rich with local minima. Therefore, we found it strictly necessary to perform molecular dynamics (MD) simulation as a prelude to final optimization of atomic positions in cases where the final atomic arrangement was not obvious or constrained. Typically, we

 0031-9007/00/85(3)/610(4)$15.00

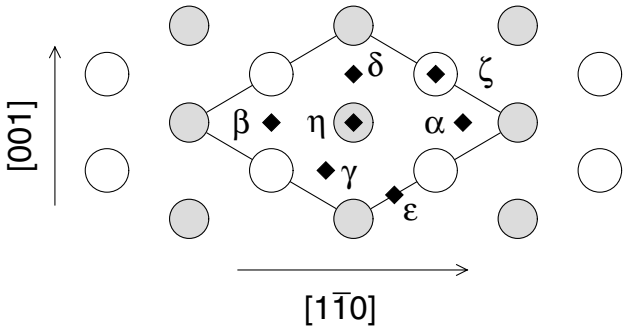

FIG. 1. Top view of the ideal NiAl(110) surface. A unit cell used in the simulations is shown with solid lines. Smaller dark circles represent Ni atoms, larger white circles Al atoms. Black diamonds mark various sites for O atom adsorption (the case of 1/3 ML coverage) and the Greek labels are as in Table I.

TABLE I. The 1/3 ML oxygen coverage: surface energy $\Delta\gamma$ (in eV/cell) relative to the energy of configuration α, and distances (in Å) between an O atom and the nearest Al ($l_{\text{O-Al}}$) and Ni atoms ($l_{\text{O-Ni}}$), and between the outermost O and Al subplanes Δd. As the number of atoms for each species is the same for all configurations, $\Delta\gamma$ on Ni- and Al-rich sides are equal.

Notation	Adsorption site	$l_{\text{O-Al}}$	$l_{\text{O-Ni}}$	Δd	$\Delta\gamma$
α	2Al + Ni hollow	1.84	1.98	0.95	0
β	Al-Al bridge	1.81	2.42	0.97	0.20 (0.05)
γ	Al + 2Ni hollow	1.80	1.95	0.93	0.59 (0.74)
δ	Ni-Ni bridge	1.98	1.97	0.67	0.59 (0.81)
ε	Al-Ni bridge	1.78	1.88	1.08	0.99 (1.02)
ζ	Al top	1.71	⋯	1.53	2.59 (2.17)
η	Ni top	⋯	1.77	1.33	3.02 (3.00)

did from 300 to 500 MD steps at $T = 1000$ K and then took the atomic configuration of lowest potential energy as a starting configuration for subsequent zero-temperature geometry optimization.

The surface free energy γ of a particular configuration is defined as [14]

$$\gamma = \frac{1}{A}\left(G - \sum_i \mu_i N_i\right) - \gamma_0^u,$$

where G is the Gibbs free energy of the whole slab, μ_i and N_i are the chemical potential and number of atoms of species i, A is the surface area, and γ_0^u denotes the surface energy of the unrelaxed (110) surface of pure NiAl. Thus we assume that any changes in atomic configurations near the surface of the slab that we use for simulations do not affect the surface energy of its other side. The chemical potentials of Ni and Al for Ni- and Al-rich NiAl alloys can be calculated in the zero-temperature limit as described in Ref. [15], the chemical potential of O has been set to zero as we shall be considering only changes in γ at fixed oxygen content.

The free NiAl(110) surface is known to ripple with the Al atoms being displaced above the Ni atoms. The magnitude of the rippling found experimentally (0.18–0.24 Å) and theoretically (0.19–0.27 Å) (see [16,17] and references therein) is well reproduced in our calculations (0.20 Å). Also the NiAl(110) surface energy (1.79 J/m^2) is similar to that obtained in other calculations: 1.87 J/m^2 [17] and 2.08 J/m^2 (unrelaxed) [18]; the experimental surface energy of liquid NiAl just above the melting temperature is 1.4 J/m^2 (see references in [19]). It should be noted that the local density approximation (LDA), which we have employed here and which has also been used in [17,18], has a tendency to overestimate surface energies in pure metals [20]. Indeed, within the generalized gradient approximation (GGA) [21] we obtained the lower surface energy (1.37 J/m^2) which is probably an underestimate. In view of the difference between these energies, in the rest of the paper we report both the LDA and GGA values (in brackets), though we stress that the picture that emerges for both sets of calculations is the same.

The study of the adsorption of one O atom per supercell (1/3 ML) [22] reveals the preferred position of the oxygen at the (2Al + Ni) hollow site above the top layer (Table I). Adsorption of O at the Al-Al bridge site is close in energy. The distances between the adsorbed O and the nearest Al atoms ($l_{\text{O-Al}}$) and between the oxygen and aluminium subplanes (Δd) are a little larger than those reported for the adsorption of an O atom at the Al(111) surface (1.79 Å and 0.7 ± 0.1 Å, respectively; see references in [2]). The LDA and GGA energies listed in Table I demonstrate the same ranking preference of O atoms to have Al rather than Ni as a nearest neighbor. It is indicative that if placed at the Ni-Ni bridge site, the O atom pushes two Ni neighbors away, while two neighboring Al atoms move closer to it. As a result, the distances $l_{\text{O-Al}}$ and $l_{\text{O-Ni}}$ become almost equal (Table I).

The strong influence of the O atoms on the structure of the substrate is even more pronounced in the case of 1 ML adsorption at the surface. After the initial oxygen adsorption at the NiAl surface having the bulk equiatomic composition in all layers (composition A), a large drop in surface energy is found either by introducing an *exchange defect* (interchanging a surface Ni atom with a subsurface Al atom, configuration G) or by absorbing a Ni vacancy in the top layer (configuration C). Note that there are two possible ways for a system to get rid of a Ni atom in the top layer (either to exchange it with Al in the second layer or to adsorb a Ni vacancy), and these are represented by configurations G and C, respectively. Encouraged by this observation, we considered both the exchange defect and the Ni vacancy in the top layer simultaneously (configuration E), and arrived at the lowest energy atomic arrangement, which is shown on Fig. 2 and demonstrates two well distinguished O and Al layers. The distance between the outermost O and Al subplanes Δd (0.63 Å) is close to that for the Al(111) surface (0.7 Å). Al atoms in the top layer arrange themselves in a distorted hexagonal packing and have almost lost their sublattice individuality; hence the

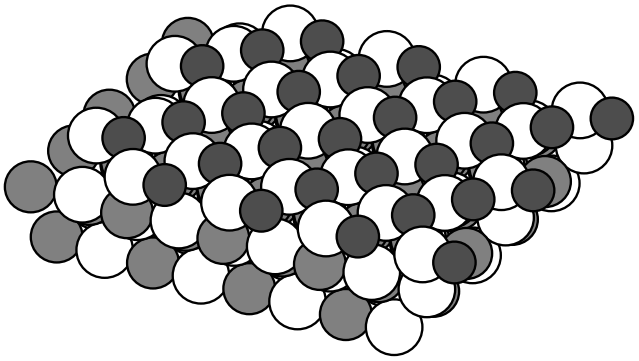

FIG. 2. The lowest in energy structure (configuration E) corresponding to the 1 ML oxygen coverage of NiAl(110). White, grey, and dark grey balls denote Al, Ni, and O atoms, respectively.

obtained O-Al bilayer could be considered as the precursor of the γ-Al_2O_3-like oxide phase. The structure of the bilayer closely resembles the lower bilayer of the alumina film in the structural model, suggested by Yang *et al.* [7].

Because configuration E requires a vacancy to be absorbed in the top layer, the actual bulk composition of the NiAl becomes important. The composition in Ni-rich and Al-rich NiAl is maintained by different constitutional defects (by nickel antisites Ni_{Al} and by nickel vacancies V_{Ni}, respectively), which give rise to different oxidation kinetics as discussed below.

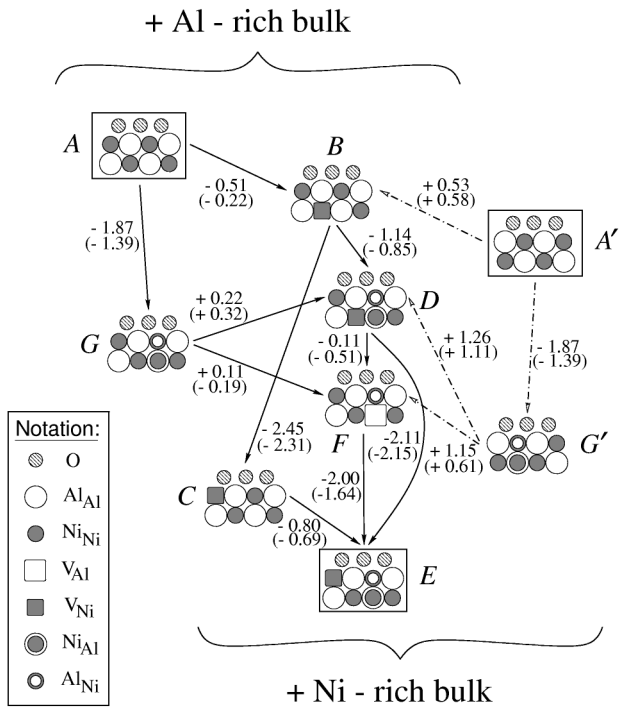

FIG. 3. Suggested pathways (marked with arrows) for the optimization of atomic positions starting from configuration A and finishing in configuration E and corresponding energy change according to LDA and GGA (in brackets) data in Al-rich NiAl. On the Ni-rich side, configurations A and G in the diagram should be replaced by A' and G'. Configurations are labeled as in Table II. The difference between the Ni-rich and Al-rich systems enters solely through the chemical potential of the components.

Consider possible pathways for the system to arrive to configuration E starting from configuration A. The pathways involving single events are depicted in Fig. 3, together with their energies. After chemisorption of 1 ML of O atoms at the perfect surface (configuration A), the system can proceed by segregating a Ni vacancy in the second layer ($A \rightarrow B$), which then may jump to the surface layer ($B \rightarrow C$), and the creation of an exchange defect ($C \rightarrow E$) completes the path $ABCE$. Alternatively, having a Ni vacancy in the second layer the system can first create an exchange defect ($B \rightarrow D$) and then either allow the Ni vacancy to jump to the first layer immediately ($D \rightarrow E$) or first convert $V_{Ni}^{(2)}$ and $Ni_{Al}^{(2)}$ defects [23] into Al vacancy $V_{Al}^{(2)}$ (i.e., the Ni antisite atom returns to its own sublattice, filling a Ni vacancy there), which is filled afterwards with a nearest-neighbor Ni atom from the first layer ($D \rightarrow F \rightarrow E$). Another family of pathways arises if we suppose that the system starts by creating an exchange defect ($A \rightarrow G$). Then a Ni vacancy arrives to the second layer either on the Ni sublattice ($G \rightarrow D$) or to the Al sublattice ($G \rightarrow F$), and the rest is the same as described above.

In Ni-rich alloys vacancies are not constitutional defects. Their creation is energetically costly, and this results in the appearance of an additional energetic barrier which enters the calculations of γ via μ_{Ni}. Indeed, on the Al-rich side each subsequent step lowers the energy of the system, with the exception of the $G \rightarrow D$ (LDA and GGA) and $G \rightarrow F$ (LDA) transitions, which are slightly uphill. On the contrary, on the Ni-rich side the transition $A' \rightarrow B$ already requires noticeable energy. The situation is even worse if the system starts with an antisite defect formation ($A' \rightarrow G'$), because this requires an even larger amount of energy to proceed further or to return to A'. Overall, on the Ni-rich side an additional 0.5 eV barrier appears for *all* the paths in comparison to the Al-rich case.

How can we rationalize the cascade of energies we find for the metastable surfaces depicted in Fig. 3? We first compared their structural parameters such as the number and length of Al-O bonds, thinking with a simple pairwise argument that a large number of Al-O bonds might favor a particular structure, or perhaps a short average Al-O bond length. These parameters gave no indication of the ranking at all. We then considered the argument (see, e.g., Ref. [24]) that a large distance between the two top layers of ions might indicate an unstable surface. The thinking here is that a neutral plane would be more characteristic of a low energy surface, whereas a bilayer of charged species, a dipole layer, would be unstable. However, this argument also fails to indicate the ranking of surface energies here; it is inappropriate to think of oxygens and metal atoms at a surface as carrying nominal charges [25]. Indeed, our

TABLE II. The 1 ML oxygen coverage: point defects present [23] and the composition of the upper NiAl layer (including oxygen) for different configurations and their surface energy $\Delta\gamma$ (in eV/cell) relative to the energy of configuration A.

Configuration	Point defects	Upper layer	$\Delta\gamma$ Ni-rich	$\Delta\gamma$ Stoichiometric	$\Delta\gamma$ Al-rich
A	none	$Ni_2Al_2O_3$	0	0	0
B	$V_{Ni}^{(2)}$	$Ni_2Al_2O_3$	+0.53 (+0.58)	+0.18 (+0.31)	−0.51 (−0.22)
D	$V_{Ni}^{(2)} + Ni_{Al}^{(2)} + Al_{Ni}^{(1)}$	$Ni_1Al_3O_3$	−0.61 (−0.28)	−0.96 (−0.54)	−1.65 (−1.07)
F	$V_{Al}^{(2)} + Al_{Ni}^{(1)}$	$Ni_1Al_3O_3$	−0.72 (−0.78)	−1.07 (−1.05)	−1.76 (−1.58)
G	$Ni_{Al}^{(2)} + Al_{Ni}^{(1)}$	$Ni_1Al_3O_3$	−1.87 (−1.39)	−1.87 (−1.39)	−1.87 (−1.39)
C	$V_{Ni}^{(1)}$	$Ni_1Al_2O_3$	−1.92 (−1.73)	−2.27 (−2.00)	−2.96 (−2.53)
E	$V_{Ni}^{(1)} + Ni_{Al}^{(2)} + Al_{Ni}^{(1)}$	Al_3O_3	−2.72 (−2.42)	−3.07 (−2.69)	−3.76 (−3.22)

lowest energy surface is a clearly resolved bilayer, with an O plane outside an Al plane, and it is certainly not the thinnest of the O-Al bilayers we are considering. Finally, the best indicator of the surface energy turns out to be the extent to which Ni has been excluded from the layer of oxide which is bonded to the substrate metal. This information is summarized in Table II, which shows how decreasing surface energy (columns 4–6) is associated with expulsion of Ni from the oxide layer into the bulk (column 3).

In conclusion, we have studied the initial stages of oxidation of the NiAl(110) surface up to 1 ML oxygen coverage. After the initial chemisorption of oxygen, significant reduction of the energy could be achieved by the co-adsorption of V_{Ni} in the first layer and by the exchange of Al and Ni atoms between the first two layers. Therefore, at the start of the oxidation process the surface must absorb vacancies rather than inject them. A change of oxidation kinetics is predicted in crossing the equiatomic composition due to the corresponding changes in chemical potentials of the species in the bulk NiAl.

We thank the EPSRC for the provision of computer time on the Cray T3E-1200E via the UKCP consortium (Grant No. M01753), and for other resources (Grant No. L08380), and we acknowledge the Centre for Supercomputing in Ireland for computer resources on the IBM SP2.

[1] H. Brune, J. Wintterlin, R. J. Behm, and G. Ertl, Phys. Rev. Lett. **68**, 624 (1992).
[2] J. Jacobsen, B. Hammer, K. W. Jacobsen, and J. K. Nørskov, Phys. Rev. B **52**, 14 954 (1995).
[3] H.-J. Freund, H. Kuhlenbeck, and V. Staemmler, Rep. Prog. Phys. **59**, 283 (1996).
[4] K. H. Hansen *et al.,* Phys. Rev. Lett. **83**, 4120 (1999).
[5] J. Libuda *et al.,* Surf. Sci. **318**, 61 (1994).
[6] R. M. Jaeger *et al.,* Surf. Sci. **259**, 235 (1991).
[7] J. C. Yang, E. Schumann, H. Müllejans, and M. Rühle, J. Phys. D **29**, 1716 (1996).
[8] H. Isern and G. R. Castro, Surf. Sci. **211-212**, 865 (1989).
[9] A. Parthasarathi and H. L. Frazer, Philos. Mag. A **50**, 101 (1984).
[10] A similar phenomenon is the possible switch of the species type which segregates to the surface in ordered alloys on either side of stoichiometry [A. V. Ruban (private communication)].
[11] A. Alavi, J. Kohanoff, M. Parrinello, and D. Frenkel, Phys. Rev. Lett. **73**, 2599 (1994).
[12] M. H. Lee, Ph.D. thesis, University of Cambridge, 1995.
[13] N. Troullier and J. L. Martins, Phys. Rev. B **43**, 1993 (1991).
[14] M. W. Finnis, Phys. Status Solidi (a) **166**, 397 (1998).
[15] M. Hagen and M. W. Finnis, Philos. Mag. A **77**, 447 (1998).
[16] J. R. Noonan and H. L. Davis, Science **234**, 310 (1986).
[17] A. T. Hanbicki *et al.,* Surf. Sci. **331–333**, 811 (1995); **365**, L639 (1996).
[18] N. I. Medvedeva *et al.,* Phys. Rev. B **54**, 13 506 (1996).
[19] D. B. Miracle, Acta Metall. Mater. **41**, 649 (1993).
[20] L. Vitos, A. V. Ruban, H. L. Skriver, and J. Kollár, Surf. Sci. **411**, 186 (1998).
[21] A. D. Becke, Phys. Rev. A **38**, 3098 (1988); J. P. Perdew, Phys. Rev. B **33**, 8822 (1986). All the GGA energies reported in the paper have been obtained using the LDA relaxed atomic configuration.
[22] We define 1 ML of adsorbed O atoms to correspond to three O atoms per each cell of the slab [four atomic sites in a NiAl(110) layer], which agrees with the structural models of the $NiAl(110)/Al_2O_3$ interface, suggested in Refs. [6,7].
[23] $X_Y^{(i)}$ denotes species X on sublattice Y in layer i, counting from the top layer of the NiAl(110) surface.
[24] D. R. Jennison, C. Verdozzi, P. A. Schultz, and M. P. Sears, Phys. Rev. B **59**, R15 605 (1999).
[25] For a discussion see, e.g., M. W. Finnis, CCP3 Newsletter, January 1999. The paper can be downloaded from http://www.cse.clrc.ac.uk/Activity/CCP3+891.